# Operation Optimization of Reconnection Marshalling Trains Considering Carbon Emission

Shixiang Wan, Changfeng Zhu, Jinhao Fang, Jie Wang, and Linna Cheng

*Abstract*—**Aiming at the problems of insufficient transport capacity of fixed marshalling trains in the peak period of passenger flow and waste of transport capacity in the off-peak period of passenger flow, the matching problem of subway passenger flow and transport capacity can be effectively solved by running reconnection marshalling trains. By considering carbon emission, the objective function is to minimize the passenger travel cost, enterprise operation cost, and carbon emission, and the prospect theory is introduced to describe the limited rationality of passenger travel path selection. The passenger flow is divided into full-length and short-turn routing, and a multi-objective optimization model for the operation scheme of reconnection marshalling trains is constructed, along with a quantum genetic algorithm designed for optimization. Taking a particular urban rail transit line as the research object, the validity and feasibility of the model and algorithm design are verified.**

*Index Terms*—**Urban rail transit, Reconnection marshalling, Carbon emission, Bounded rationality, Quantum genetic algorithm**

## I. Introduction

The whole-day passenger flow time distribution of urban rail transit has obvious "tidal" characteristics, and the traditional fixed marshalling mode can no longer achieve a high matching between passenger flow and transport capacity. Therefore, a hot research topic in the field of urban rail transit is the optimization of flexible train formation. One of the flexible marshalling operation organization modes is the reconnection marshalling operation organization mode. In order to improve the uneven utilization rate of trains and the mismatch between passenger flow and transport capacity, the reconnection marshalling trains are operated in the transition phase of double-peak passenger flow (peak and off-peak periods). In view of the dynamic change of rail transit passenger flow demand with time and the unbalanced spatial distribution, relevant scholars have studied the urban rail operation scheme to achieve a good match between passenger flow and vehicle flow.

In earlier studies, [1] put forward the operation scheme of flexible marshalling and analyzed its technical feasibility, advantages, and disadvantages. [2] analyzed the three combined transportation organization modes and operation characteristics of flexible marshalling and collinear operation, flexible marshalling and multi routing, and flexible marshalling and fast and slow train operation. [3] built a multi-objective optimization model of train operation scheme based on flexible marshalling and designed a four-stage algorithm to solve the problem of unbalanced daily passenger flow time distribution. [4] built a model to obtain the setting of each traffic organization parameter with the least number of train groups. [5] described the total waiting time of passengers at the minimum station by calculating and adjusting the railway train schedule with a given variable starting point to the terminal passenger demand matrix. [6] combined and optimized the train schedule with the train bottom connection plan to reduce the train operation cost. [7] put forward the minimum objective model of the total travel time of passengers. [8] proposed a new strategy-level collaborative optimization method for train stop planning and train scheduling. [9] proposed a multi-train energy-saving operation strategy suitable for various line conditions and complex train schedules. [10] proposed a train set cycle optimization model to minimize the total connection time and maintenance cost. [11] proposed a mixed integer programming model to solve the train scheduling problem on two-way urban subway lines. [12] studied the problem of train formation and proposed an accurate dynamic programming algorithm based on the inclusion-exclusion principle to split the train formation. [13] discussed the relationship between the walking distance to the subway station and the demographic characteristics of passengers, providing an important reference for planners and transport departments to optimize land use and transport infrastructure. After analyzing the components of the total travel time of passengers. [14] studied the dynamic characteristics of passenger flow demand and the characteristics of train departure headway under full-length and short-turn routing modes and designed algorithms to solve the passenger flow demand of each station in any time period. [15] built a variable multi-objective optimization model for train formation and optimized the operation scheme of full-length and short-turn routing to solve the problem of passenger flow difference at sections. [16] studied how to optimize the fixed

Manuscript received October 25, 2022; revised April 2, 2023.

This work was supported in part by the National Natural Science Foundation of China (No. 72161024), “Double-First Class” Major Research Programs, Educational Department of Gansu Province (No. GSSYLXM-04) and Gansu Provincial Science and Technology Plan Project (22ZY1QA005).

Shixiang Wan is a postgraduate student at School of Traffic and Transportation, Lanzhou Jiaotong University, Lanzhou 730070, China. (e-mail: 13541950798@163. com).

Changfeng Zhu is a Professor at School of Traffic and Transportation, Lanzhou Jiaotong University, Lanzhou 730070, China. (e-mail: cfzhu003@163. com).

Jinhao Fang is a PhD candidate at School of Traffic and Transportation, Lanzhou Jiaotong University, Lanzhou 730070, China. (e-mail: fangjin_hao@163. com).

Jie Wang is a PhD candidate at School of Traffic and Transportation, Lanzhou Jiaotong University, Lanzhou 730070, China. (e-mail: 1009696615@qq. com).

Linna Cheng is a PhD candidate at School of Traffic and Transportation, Lanzhou Jiaotong University, Lanzhou 730070, China. (e-mail: chengjj2021@163. com).

marshalling into flexible marshalling, achieve "large marshalling and high-density" operation during peak passenger flow periods, and achieve "small marshalling and high-density" operation during non-peak passenger flow periods, balancing the contradiction between transport capacity and service level. According to passenger flow distribution and the characteristics of full-length and short-turn routing trains operating on the same line. [17] analyzed the mechanism of passenger distribution on the platform, and the research results will help the subway operation planners and station staff to take measures to manage passenger distribution on the platform. [18] dynamically assigned passengers to competent trains. [19] put forward a coordinated optimization method of transportation organization combining full-length and short-turn routing schemes with multi-station joint flow restriction to solve the problems such as uneven distribution of passenger flow, mismatched supply and demand capacity, and high safety pressure of large passenger flow at stations during urban rail peak hours. [20][21][22] studied the multi-formation of urban rail transit and solved the problems of train operation, train capacity, and variable full load rate of large and small formations. Some scholars have studied the problem of train operation from the technical level. [23][24][25] studied the full-length and short-turn routing of urban rail transit and solved the problems of train operation, balance of full load rate, and operation proportion.

Scholars in recent research, [26] generated a set of alternative routes, built a service network according to the layout of turn-back stations on the line, used the optimal strategy to allocate passenger flow to the service network, and described the passenger's choice behavior for trains with different routes. [27] provided theoretical support and a decision-making basis for subway operation departments to formulate passenger flow control strategies by reducing travel costs and alleviating overcrowding. [28] studied the train organization problem of small-scale subway networks during peak hours and comprehensively considered the economic cost, capacity utilization, and transmission coordination. [29] studied the problem of additional train paths in multi-objective optimization and short-term planning applications to minimize the total adjustment of initial trains and the number of required train sets. In order to solve the leftover phenomenon and passenger selection behavior. [30] deduced the optimal schedule design of multi-phase demand of two-way rail transit lines and solved the problems of minimum passenger and total operation cost and reliability of train formation. [31] proposed an accurate dynamic programming algorithm to solve the problem of reordering rail vehicles by rail lines. [32] introduced the specific flexible marshalling scheme, functional requirements, and their implementation, and analyzed the economic benefits of the operation of 3-car marshalling trains in the flat peak period. It has laid a technical and theoretical foundation for our research on multiple marshalling. [33] proposed an accurate mixed integer programming model to optimize the cycle skip mode of fast trains running in the monorail metro system. [34] proposed a two-stage stochastic programming model based on flexible marshalling of urban rail car bottom operation plan and robust passenger flow control strategy to solve the imbalance problem of commuter passenger flow demand. [35] built a two-level planning model considering a multi-marshalling urban rail train cross-line operation plan to solve the problems of uneven utilization of transport capacity and significant differences in total load rate between cross-line and non-crossline trains due to different train service levels under the cross-line operation mode. [36] based on the characteristics of flexible marshalling operation organization mode, comprehensively considered the competitive relationship between passenger flow and freight flow, built a model solution algorithm to obtain the train marshalling scheme, train diagram, and passenger freight coordinated transportation scheme. [37] proposed a collaborative optimization method of urban rail transit timetable and underbody utilization plan considering full-length and short turn routing, so as to reduce the difficulty of preparing timetable and underbody utilization plan for urban rail transit full-length and short turn routing. [38] built a multi-objective nonlinear routing scheme optimization model to solve the carbon emission optimization problem of urban rail trains, taking passenger travel cost, carbon emission of train operation, and enterprise operation cost as optimization objectives. [39] built an urban rail timetable optimization model considering the energy saving of train operation and the use of vehicle bottom, and solved the model with an efficient particle swarm algorithm to solve the urban rail timetable optimization problem of train operation energy consumption and the use of vehicle bottom.

To sum up, few theories on urban rail transit reconnection marshalling have been proposed, most of which focus on the research of fixed marshalling and only a small number of studies on multi-marshalling and flexible marshalling. The existing studies are all based on the assumption that passengers are entirely rational, ignoring the limited rational behavior of passengers, and rarely take carbon emission as the optimization target in selecting objective functions. Based on this, this paper takes the urban rail transit reconnection marshalling trains as the research object and takes the spatial and temporal distribution imbalance of the whole day passenger flow as the starting point to study the operation scheme of reconnection marshalling trains. Large marshalling trains will be operated during the peak passenger flow period, while small marshalling trains will be operated during the peak passenger flow period, and large marshalling trains and small marshalling trains will run together during the bimodal transition period. At the same time, in addition to the passenger travel cost and the enterprise operation cost, the carbon emission is included into the optimization goal, and the prospect theory is introduced to depict the limited rationality of passenger travel path selection, providing a basis for the green and efficient urban rail reconnection marshalling operation optimization.

The rest of this paper is summarized as follows: Section II describes the problem studied in mathematical language. Based on the analysis in Section II, the model of the operation scheme of the reconnection marshalling is established in Section III. Section IV designs a case verifies the rationality of the model constructed in Section III, and analyzes the influence of some parameter changes on the results. Finally, the conclusion of this paper is in Section V.

## II. PROBLEM DESCRIPTION

Reconnection marshalling is one of the flexible marshalling operation modes of subway, which can effectively improve the matching degree of subway passenger flow demand and capacity configuration. The double marshalling operation mode refers to the marshalling mode in which large marshalling trains need to be disassembled into small marshalling trains or two small marshalling trains need to be reconnected into a large one in order to improve the uneven utilization of trains during the double peak passenger flow (peak and off-peak periods) transition phase. The operation mode diagram of reconnection marshalling is illustrated in Fig.1.

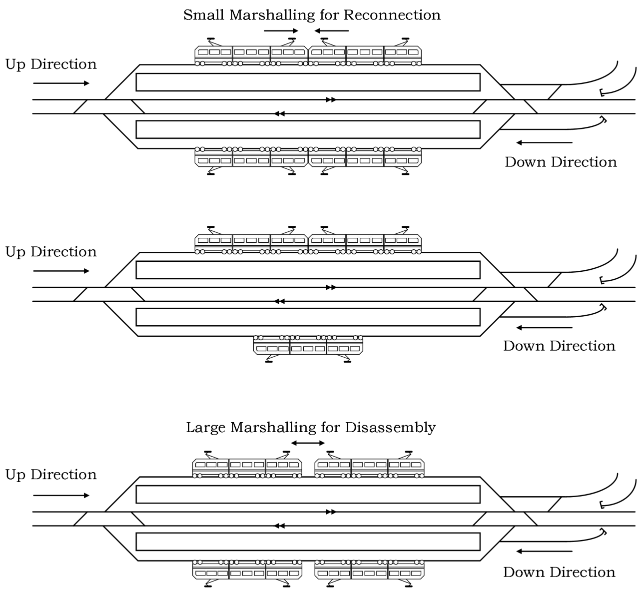


Fig.1. Operation Mode of Reconnection marshalling

Suppose L is an urban rail transit line, let $S=\{s|s=1,2,\cdots,N+1,\cdots 2N\}$ be the station set. Full day operation duration is $T$ , $T=\{T_r|r=1,2,\cdots,H\}$ .The interval is marked as $Y$ , $Y=\{Y_y|y=1,2,\cdots,N-1\}$ . $d$ defines as $d=1$ for up direction and $d=2$ for down direction.; Reconnection marshalling train is marked as $m$ with $m=1$ denotes small marshalling and $m=2$ denotes large marshalling. $e$ indicates train routing, when $e=1$ it is indicated small routing, when $e=2$ indicates large routing. Let $B=\{b_m^r\}$ be the train formation type set, where $b_m^r$ refers to the number of train formation type $m$ during time period $T_r$ . $b^{'}$ and $b^{''}$ represent the upper limit and lower limit of the number of train marshalling vehicles respectively $E$ is the train capacity. $\varpi_1$ is the cost of purchasing trains. $\varpi_2$ is the running cost per kilometer. $U=\{u_{m,d}|m=1,2,d=1,2\}$ defines train symbol, where $u_{2,d}=\{u_{1,d}+u_{1,d}\}$ 。 $\eta$ is the ratio of departure frequency of large and small routing trains, and $\eta=\left(f_1^{r,1}+f_1^{r,2}\right)/\left(f_2^{r,1}+f_2^{r,2}\right)$ . $V_d$ is the traveling speed of the train in the direction $d$ . $T_z$ is turning back time. $f_e^{r,m}$ refers to the departure frequency of train with $e$ routing and $b_m^r$ marshalling quantity $T_r$ in time segment. $t_{i,operate}$ is the running time of train section. $t_{i,stop}$ is the actual dwell time of the train. $K=\{k|k=1,2,\cdots,K\}$ indicates the effective path of each OD。 $q_{ij}^{r,k}$ refers to the passenger flow of the $k$ -th route from station $i$ to station $j$ during time period $r$ . $t_r^k$ refers the running time of the train in route $k$ . $t_{S_{stop}}^k$ represents the dwell time of the train outside the departure and destination stations at the station of route $k$ . $\vartheta_e$ is 1 if routing $e$ is selected, otherwise it is 0. $M$ donates a large enough number. $\varepsilon_{ij}^k$ represents random error, and $E\left(\varepsilon_{ij}^k\right)=0$ 。 $w^+\left(p_{ij}^k\right)$ and $w^-\left(p_{ij}^k\right)$ represent the subjective probability of passengers choosing path $k$ when the travel time of path $k$ between station $i$ and station $j$ is less than or greater than the reference time. $L_1$ is the small routing distance. $L_2$ is the large routing distance. $CeO$ is the total carbon emission in the subway operation stage. $P_{subway}$ is the traction power consumption of metro train. $P_{station}$ is the power and lighting power consumption of metro station. $E_{k,e}$ is the electric power emission factor. $P_\mu$ is the adhesion mass of the vehicle. $g$ is the acceleration of gravity. $P_F$ is the traction power of the train. $A,B,C$ are the empirical coefficients of basic resistance.

To sum up, operation scheme $\psi$ of urban rail reconnection marshalling trains can be represented as $\psi=\{S,T,B,U,f_e^{r,m}\}$.

## III. MODEL COSTRUCTION

To simplify the problem, it is assumed that passengers arrive at the station evenly, obeying first come, first served principle, and there is no reservation and relevant facilities such as turn back station, marshalling and unmarshalling station, and depot meets the requirements of running reconnection marshalling trains. The specific model is as follows:

### *A. Objective Function*

#### *A.1. Considering the travel cost of passengers with limited rationality*

The passenger flow is allocated with bounded rationality [40], and travel time of passengers is the influencing factor for route selection. In the process of taking urban rail trains, passengers' travel time includes three parts: waiting time at the departure station, interval operation time, and transfer time. That is to say, passengers decide whether to choose a route according to the travel time cost. The travel time cost of passengers is calculated as follows.

Because the tracking interval of subway trains is short, the arrival of passengers can be considered independent of the train schedule, showing the characteristics of random normal distribution. According to statistics, the waiting time of subway passengers at the departure station is considered half of the train departure interval, as shown in (1):

$$t_{ij}^{k,wait} = \frac{T}{2\cdot\left(f_e^{r,m}\right)} \tag{1}$$

The running time of passengers in the section can be divided into running time of the train and the dwell time of the train at each station, as shown in (2):

$$t_{ij}^{k,operate} = \sum_{r=T_r} t_r^k + \sum_{S_{stop\in S}} t_{S_{stop}}^k \tag{2}$$

Passenger transfer time consists of travel time and waiting time. Considering that passengers transfer through the same platform for a single line, travel time is not considered and only waiting time is counted, as shown in (3):

$$t_{ij}^{k,transfer} = \sum_{r\in T_r}\sum_{e=1}^{2}\sum_{m=1}^{2}\left[\left(1-\vartheta_e\right)\cdot M + \frac{2T}{f_e^{r,m}}\right] \tag{3}$$

Then the time cost function of passengers traveling through path $k$ from station $i$ to station $j$ is as follows (4):

$$T_{ij}^k = t_{ij}^{k,wait} + t_{ij}^{k,operate} + t_{ij}^{k,transfer} + \varepsilon_{ij}^k \tag{4}$$

Set the average running time of all paths of each OD as the reference point in the value function, as shown in (5):

$$T_{ij}^0 = \frac{\sum_{k=1}^{K} T_{ij}^k}{K} \tag{5}$$

When the travel time cost is less than the reference point, it means the gain; when it is greater than the reference point, it means the loss. Therefore, the value function of route $k$ between station $i$ and station $j$ is shown in (6), and the value function curve of route $k$ between station $i$ and station $j$ is illustrated in Fig.2.

$$v\left(T_{ij}^k\right) = \begin{cases} v^+\left(T_{ij}^k\right) = \left(T_{ij}^0 - T_{ij}^k\right)^{\chi}, & T_{ij}^0 \ge T_{ij}^k \\ v^-\left(T_{ij}^k\right) = -\lambda\left(T_{ij}^k - T_{ij}^0\right)^{\sigma}, & T_{ij}^0 < T_{ij}^k \end{cases} \tag{6}$$

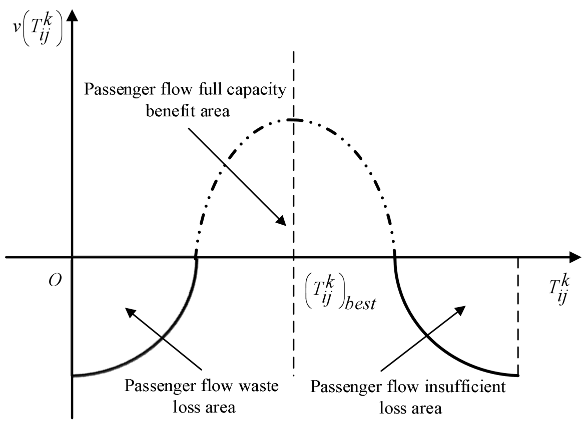


Fig.2. Time Value Function Curve

Taking the average travel time of all paths of each OD as the reference point. Assuming that $\varepsilon_{ij}^k$ is independent of each other and follows Gumbel distribution, then the *MNL* (*Multinational Logit*) model can be introduced as the objective passenger flow distribution proportion of route $k$ from station $i$ to station $j$, as shown in (7):

$$p_{ij}^k = \frac{exp\left(v\left(T_{ij}^k\right)\right)}{\sum_{k=1}^{K} exp\left(v\left(T_{ij}^k\right)\right)}, \forall k \in K \tag{7}$$

Since decision-makers tend to overestimate low probability events and underestimate high probability events when making decisions, the subjective probability of passengers choosing route $k$ is shown in (8), and the curvature diagram of weight function is determined by the values of $\gamma$ and $\delta$ of route $k$ between stations $i$ and $j$, as shown in Fig.3.

$$w\left(p_{ij}^k\right) = \begin{cases} w^+\left(p_{ij}^k\right) = \dfrac{\left(p_{ij}^k\right)^{\gamma}}{\left[\left(p_{ij}^k\right)^{\gamma} + \left(1-p_{ij}^k\right)^{\gamma}\right]^{\frac{1}{\gamma}}} \\ w^-\left(p_{ij}^k\right) = \dfrac{\left(p_{ij}^k\right)^{\delta}}{\left[\left(p_{ij}^k\right)^{\delta} + \left(1-p_{ij}^k\right)^{\delta}\right]^{\frac{1}{\delta}}} \end{cases} \tag{8}$$

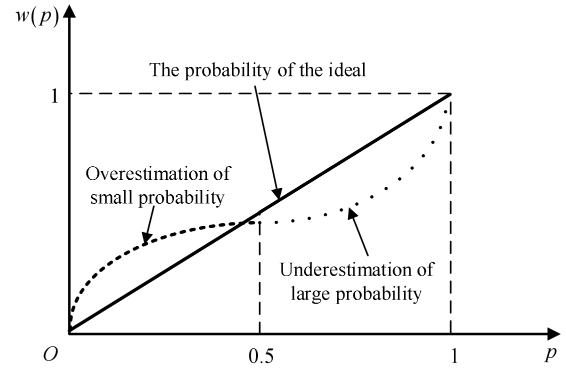


Fig.3. The value of $\gamma$ and $\delta$ are determined the weight function

$p_{ij}^k$ represents the objective probability of passengers choosing route $k$, so the foreground value of route $k$ is shown in (9):

$$V_{ij}^k = v^+\left(T_{ij}^k\right)\cdot w^+\left(p_{ij}^k\right) + v^-\left(T_{ij}^k\right)\cdot w^-\left(p_{ij}^k\right) \tag{9}$$

The actual distribution proportion of path $k$ between station $i$ and station $j$ is shown in (10):

$$P_{ij}^k = \frac{exp\left(V_{ij}^k\right)}{\sum_{k=1}^{K} exp\left(V_{ij}^k\right)}, \forall k \in K \tag{10}$$

The travel time cost of passengers is represented by the waiting time, interval operation time, and transfer time of passengers at the departure station. The time cost corresponding to all types of passenger flows is added as well. In order to convert time cost into travel cost, considering that passenger travel time does not belong to working time, non-working time value is used to measure passenger time value, then passenger travel time cost $W_1$ of each route $k$ from station $i$ to station $j$ can be formulated as (11):

$$\min W_1=\sum_{r\in T_r}\sum_{k=1}^{K}\sum_{i=1}^{S-1}\sum_{j=2}^{S}q_{ij}^{r,k}\cdot\left(t_{ij}^{k,wait}+t_{ij}^{k,operate}+t_{ij}^{k,transfer}\right)\quad(11)$$

*A.2. Enterprise operating cost*

The enterprise operation cost mainly includes the train purchase cost and the train operation cost. The enterprise operation cost $W_2$ (14) can be divided into the train purchase cost $\xi_1$ (12) and the train operation cost $\xi_2$ (13):

$$\xi_1=\frac{\varpi_1}{T}\cdot\frac{\eta}{3600}\cdot\left[\begin{array}{l}\left(f_1^{r,1}+f_1^{r,2}\right)\cdot\left(\sum_{i=a}^{b}t_{i,operate}+\sum_{i=a}^{b}t_{i,stop}+2T_z\right)+\\\left(f_2^{r,1}+f_2^{r,2}\right)\cdot\left(\sum_{i=1}^{N}t_{i,operate}+\sum_{i=1}^{N}t_{i,stop}+2T_z\right)\end{array}\right]\quad(12)$$

$$\xi_2=\varpi_2\cdot V_d\cdot\frac{\eta}{3600}\cdot\left[\begin{array}{l}\left(f_1^{r,1}+f_1^{r,2}\right)\cdot\left(\sum_{i=a}^{b}t_{i,operate}+\sum_{i=a}^{b}t_{i,stop}+2T_z\right)+\\\left(f_2^{r,1}+f_2^{r,2}\right)\cdot\left(\sum_{i=1}^{N}t_{i,operate}+\sum_{i=1}^{N}t_{i,stop}+2T_z\right)\end{array}\right]\quad(13)$$

$$\min W_2=\xi_1+\xi_2\quad(14)$$

*A.3. Carbon emission*

As the most extended period in the whole cycle of the subway, the subway operation consumes a large amount of energy. Energy consumption in the metro operation stage mainly includes train traction energy consumption and station (including depot) operation energy consumption. In this paper, the carbon emission in the subway operation phase mainly focuses on the impact of energy consumption during train acceleration traction and environmental control systems, station power equipment, lighting equipment, and other equipment. It is worth noting that the energy consumption during subway operation is mainly electricity consumption. Therefore, this paper only considers the carbon emission generated by the power consumption in the subway operation stage. The calculation method [41] is shown in (15).

$$CeO=P_{subway}\cdot E_{k,e}+P_{station}\cdot E_{k,e}\quad(15)$$

This paper considers the energy consumption of subway traction. Ventilation, air conditioning, lighting, and escalator account for 80% of the total power consumption of the station. The power consumption is relatively fixed and does not change due to different train operation schemes, so $P_{station}=0$. The traction power of the train is solved by the kinematics method. The work done by the train in operation is calculated by the product of the adhesion traction force, basic resistance, and the running distance of the train. The calculation (16) and (17) are as follows:

$$P_F=\left[P_\mu\cdot g\cdot\left(0.24+\frac{12}{100+8\times V_d}+A+B\cdot V_d+C\cdot V_d^{\,2}\right)\right]\cdot\left[L_1\cdot\left(f_1^{r,1}+f_1^{r,2}\right)+L_2\cdot\left(f_2^{r,1}+f_2^{r,2}\right)\right]\cdot\frac{\eta}{3600}\quad(16)$$

$$P_{subway}=P_F\cdot\sum_{r=1}^{H}T_r\quad(17)$$

To sum up, the calculation (18) of urban rail transit carbon emission $W_3$ is:

$$\min W_3=P_F\cdot E_{k,e}\cdot\sum_{r=1}^{H}T_r\quad(18)$$

*A.4. Constraints*

(1) Constraints on the minimum departure frequency of the line. The departure frequency $f_2^{r,1},f_2^{r,2}$ of large routing shall not be less than the minimum departure frequency $f_{\min}$. As shown in (19).

$$f_2^{r,1}+f_2^{r,2}\geq f_{\min}\quad(19)$$

(2) Constraints on the maximum passing capacity of the line. Set the maximum departure frequency $f_{\max}$ of the line. As shown in (20).

$$f_1^{r,1}+f_1^{r,2}+f_2^{r,1}+f_2^{r,2}\leq f_{\max}\quad(20)$$

(3) Line maximum load factor constraint. As shown in (21).

$$\varphi=\frac{\max\left\{p_x\,\middle|\,x=1,2,\cdots,X\right\}}{E\cdot f_x}\quad(21)$$

Where, $\varphi$ is the maximum load factor. $p_x$ is the section passenger flow of section $x$. When $\max\left(p_x\right)$ is in small routing section, $f_x=f_1^{r,1}+f_1^{r,2}$, and $\max\left(p_x\right)$ is in large routing section, $f_x=f_2^{r,1}+f_2^{r,2}$.

(4) Turn back station selection constraint. As shown in (22).

$$1\leq S_a<S_b\leq N\quad(22)$$

(5) Train formation quantity constraint. As shown in (23).

$$b^{'}\leq b_m^r\leq b^{"},m=1,2\quad(23)$$

(6) Constraints of train set connection relationship.

When the downlink trains $u_{1,2}$ and $u_{2,2}$ run from the starting station $N+1$ to the terminal station $2N$, three options are available:

①The train set enters the depot and ends the multiple and unmarshalling operation of the day. That is, no marshalling and unmarshalling of other trains will be carried out subsequently. Operation condition 1 of the marshalling and unmarshalling train set is illustrated in Fig.4.

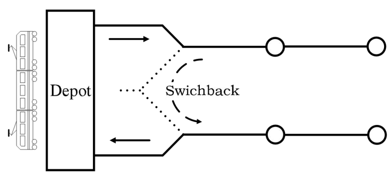


Figure.4. Operation condition of marshalling and decoupling train set 1

②The train set enters the depot but then comes out of the depot again to be reconnected and uncoupled to other trains. The operation of the reconnected and uncoupled train set 2 is illustrated in Fig.5.

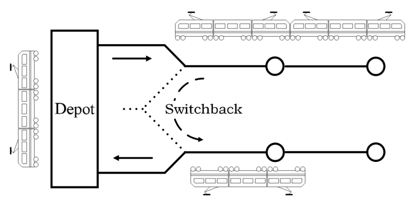


Fig.5. Operation condition of marshalling and decoupling train set 2

③After turning back directly at station $2N$, the train set continues to recouple and un-marshal an uplink train. The operation of recouple and un-marshal train set 3 is illustrated in Fig.6.

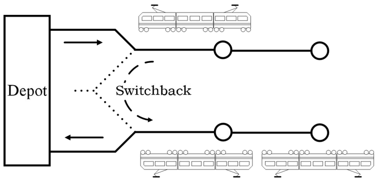


Fig.6. Operation condition of marshalling and decoupling train set 3

In order to describe the arrangement of the train set after the train set is reconnected with the down train $u_{1,2}$, and the down train $u_{2,2}$ is unmarshalled and arrives at station $2N$, for the up trains $u_{1,1}$ and $u_{2,1}$ running from station 1 to station $N$, since there is no depot where the train bottom stays at station $N$, the responsible train set can only be reconnected and unmarshalled with the next down train back to station 1 after the station turns back. Define three 0-1 variables $\alpha_{u_{m,2}u_{m,1}}$、$\beta_{u_{m,2}u_{m,1}}$、$\alpha_{u_{m,1}u_{m,2}}$, As shown in (24), (25), (26):

$$\alpha_{u_{m,2}u_{m,1}} = \{1,0\} \tag{24}$$

$$\beta_{u_{m,2}u_{m,1}} = \{1,0\} \tag{25}$$

$$\alpha_{u_{m,1}u_{m,2}} = \{1,0\} \tag{26}$$

Where, $\alpha_{u_{m,2}u_{m,1}} = 1$ indicates that the train set is reconnected and uncoupled to the down train $u_{1,2}$, $u_{2,2}$ indicates that the turn back operation is carried out at station $2N$ and the recoupled and uncoupled to the up train $u_{1,1}$, $u_{2,1}$, $\alpha_{u_{m,2}u_{m,1}} = 0$ indicates others. $\beta_{u_{m,2}u_{m,1}} = 1$ indicates that the train set is reconnected and uncoupled, the down train $u_{1,2}$ enters the depot after $u_{2,2}$, and the out section is reconnected and uncoupled on the up train $u_{1,1}$, $u_{2,1}$, $\beta_{u_{m,2}u_{m,1}} = 0$ indicates others. $\alpha_{u_{m,1}u_{m,2}} = 1$ indicates that the train set is reconnected and uncoupled to the up train $u_{1,1}$, and after $u_{2,1}$, station $N$ conducts turn back operation and is reconnected and uncoupled to the down train $u_{1,2}$, $u_{2,2}$, $\alpha_{u_{m,1}u_{m,2}} = 0$ indicates others.

Selection of up train $u_{1,1}$, $u_{2,1}$ and down train $u_{1,2}$, $u_{2,2}$ in the section:

①For any up train $u_{1,1}$ and $u_{2,1}$, after arriving at station $N$, its train set needs to connect with a down train $u_{1,2}$, $u_{2,2}$ and return to station $2N$, that is, (27) is satisfied. The selection of up train 1 is illustrated in Figure 7.

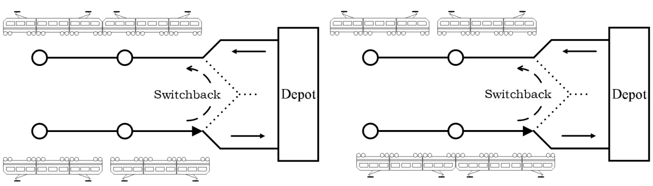


Fig.7. Selection of Up Train 1

$$\sum_{u_{m,2}} \alpha_{u_{m,1}u_{m,2}} = 1, \forall u_{m,1} \tag{27}$$

②The train set of any up train $u_{1,1}$ and $u_{2,1}$ can be from the train set that comes out of the depot for the first time, or from the train set that turns back after a down train $u_{1,2}$ and $u_{2,2}$ is reconnected and unmarshalled, or comes out of the depot after entering the depot, that is, (28) is satisfied. The selection of up train 2 is illustrated in Fig.8.

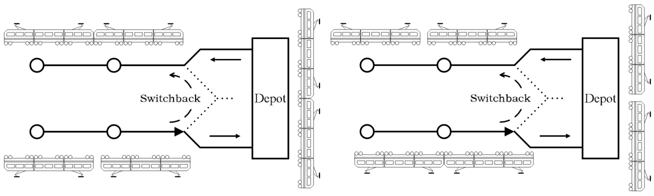


Fig.8. Selection of Up Train 2

$$\sum_{u_{m,2}} \alpha_{u_{m,2}u_{m,1}} + \sum_{u_{m,2}} \beta_{u_{m,2}u_{m,1}} = 1, \forall u_{m,1} \tag{28}$$

③For any down train $u_{1,2}$ and $u_{2,2}$, since the terminal station $2N$ it arrives at is connected with the depot, after the train is reconnected and unmarshalled, its corresponding train group can enter the depot for marshalling and unmarshalling, or turn back, or enter the depot and then exit the depot, (29) is satisfied. The selection of down train 1 is illustrated in Fig.9.

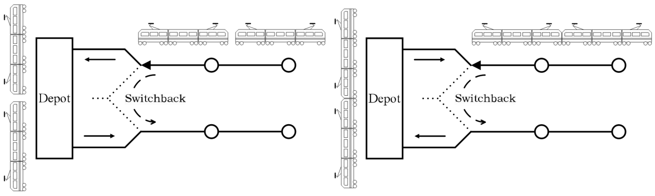


Figure.9. Selection of Down Train 1

$$\sum_{u_{m,1}} \alpha_{u_{m,2}u_{m,1}} + \sum_{u_{m,1}} \beta_{u_{m,2}u_{m,1}} \le 1, \forall u_{m,2} \tag{29}$$

④The train sets of the down trains $u_{1,2}$ and $u_{2,2}$ of the marshalling and unmarshalling can only come from the train sets that turn back after the up trains $u_{1,1}$ and $u_{2,1}$ of the marshalling and unmarshalling, that is, (30) is satisfied. The selection of the down trains is illustrated in Fig.10.

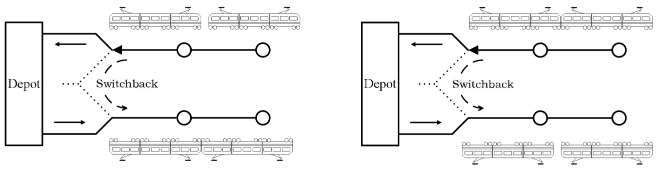


Fig.10. Selection of Down Train 2

$$\sum_{u_{m,1}} \alpha_{u_{m,1}u_{m,2}} = 1, \forall u_{m,2} \tag{30}$$

(7) Train marshalling time constraint

$T_{enter}$, $T_{exit}$ are represented the time required for the train set to enter and leave the depot, $t_{u_{m,1}}^{N_{reach}}$ and $t_{u_{m,1}}^{N_{departure}}$ are respectively represented the time when the up trains $u_{1,1}$ and

$u_{2,1}$ arrive at and leave station $N$ ,。 $t_{u_{m,2}}^{N_{reach}}$ and $t_{u_{m,2}}^{N_{departure}}$ are respectively represented the time when the down trains $u_{1,2}$ and $u_{2,2}$ arrive at and leave station $N$ .

① For the down train $u_{1,2}$ , $u_{2,2}$ running from station $N+1$ to station $2N$ , whether its train set can directly conduct turn back operation at station $2N$ and continue to be reconnected and uncoupled to the up train $u_{1,1}$ , $u_{2,1}$ depends on whether the interval time between the two workshops meets the limit of the turn back time of the train set, as shown in (31).

$$\begin{aligned}&T_{z(2N)}^{\min}\cdot\alpha_{u_{m,2}u_{m,1}}+M\cdot\left(\alpha_{u_{m,2}u_{m,1}}-1\right)\le\left[t_{u_{m,1}}^{(1)_{reach}}-t_{u_{m,2}}^{(2N)_{departure}}\right]\\&\le T_{z(2N)}^{\max}\cdot\alpha_{u_{m,2}u_{m,1}}+M\cdot\left(1-\alpha_{u_{m,2}u_{m,1}}\right),\forall u_{m,1},u_{m,2}\end{aligned}\quad(31)$$

②At station $2N$ , whether the train sets of the down trains $u_{1,2}$ and $u_{2,2}$ can exit the depot after entering the depot and be recoupled and uncoupled to the up trains $u_{1,1}$ and $u_{2,1}$ depends on whether the interval time between them meets the time limit required for entry and exit, as shown in (32).

$$\begin{aligned}&t_{u_{m,1}}^{(1)_{reach}}-t_{u_{m,2}}^{(2N)_{departure}}\le\left(T_{enter}+T_{exit}\right)\cdot\beta_{u_{m,2}u_{m,1}}\\&+M\cdot\left(\beta_{u_{m,2}u_{m,1}}-1\right),\forall u_{m,1},u_{m,2}\end{aligned}\quad(32)$$

③ For the up train $u_{1,1}$ , $u_{2,1}$ running from station 1 to station $N$ , the train set at station $N$ can only turn back and return to station $2N$ . Therefore, whether the train set can be reconnected and uncoupled to the down train $u_{1,2}$ , $u_{2,2}$ after turn back depends on whether the interval time between the two workshops meets the limit of the turn back time of the train set, as shown in the (33).

$$\begin{aligned}&T_{z(N)}^{\min}\cdot\alpha_{u_{m,1}u_{m,2}}+M\cdot\left(\alpha_{u_{m,1}u_{m,2}}-1\right)\le\left[t_{u_{m,2}}^{(N+1)_{reach}}-t_{u_{m,1}}^{(N)_{departure}}\right]\\&\le T_{z(N)}^{\max}\cdot\alpha_{u_{m,1}u_{m,2}}+M\cdot\left(1-\alpha_{u_{m,1}u_{m,2}}\right),\forall u_{m,1},u_{m,2}\end{aligned}\quad(33)$$

In equation : $M$ is a large enough positive number; $T_{z(N/2N)}=\left\{T_{z(N)}^{\max},T_{z(N)}^{\min},T_{z(2N)}^{\max},T_{z(2N)}^{\min}\right\}$ are represented the maximum and minimum turn back time of the train set at station $N$ and $2N$ respectively.

(8) Positive integer constraint. As shown in (34).

$$f_1^{r,1},f_1^{r,2},f_2^{r,1},f_2^{r,2},a,b\in Z^*\quad(34)$$

*B. Algorithm Design*

*B.1. Combination of Quantum Computing and Genetic Algorithm*

Genetic algorithm [42] has strong robustness, but it has some limitations, including slow convergence, too many iterations, easy to premature convergence and easy to fall into the local optimal solution.

Quantum computing has the parallelism of quantum mechanics and the computational speed is faster. At the same time, there are various quantum states, so it is rare to fall into the local extreme value when searching for the optimal solution.

Quantum genetic algorithm introduces quantum state vector into genetic algorithm and applies the probability amplitude of quantum bit to chromosome coding. A chromosome is a superposition of marshalling quantum states, and uses quantum revolving gates to achieve chromosomal variation renewal.

Therefore, quantum genetic algorithm has the advantages of fewer iterations, fast running speed, genetic variation with fewer populations, wide search range, and difficulty in falling into local extreme value.

*B.2. Operation steps of quantum genetic algorithm*

(1) Chromosome length calculation

In order to dynamically adjust the operation speed of the algorithm and further improve the operation efficiency, adaptive chromosome length is adopted here. The calculation method is as follows:

① Set the initial value of chromosome length $L$ as a smaller number;

②Solve the fitness function to obtain the minimum fitness $f_{\min}\left(z\right)$ and maximum fitness $f_{\max}\left(z\right)$ under the current conditions, and then obtain the calculation accuracy $\varepsilon=\frac{f_{\max}\left(z\right)-f_{\min}\left(z\right)}{2^L}$ of this operation;

③Compare the calculation accuracy with the previously preset allowable calculation accuracy $tolerance$ . If $\varepsilon>tolerance$, the current chromosome length f is increased by 1, and then return to step ②. On the contrary, the current chromosome length is the appropriate chromosome length.

(2) Quantum bit coding

Quantum computing is mainly accomplished through quantum bits. As an information carrier, quantum bits are a special two state system, which can be in the superposition state of two different quantum states at the same time, such as $\left|\varpi_q\right\rangle=\alpha\left|0\right\rangle+\beta\left|1\right\rangle$ , where $\left|0\right\rangle$ and $\left|1\right\rangle$ represent the spin down and spin up states respectively, and the probability amplitude constant $\left(\alpha,\beta\right)$ satisfies the normalization condition as shown in (35):

$$\left|\alpha\right|^2+\left|\beta\right|^2=1\quad(35)$$

The results of chromosome coding by quantum bits are shown in (36) and (37):

$$P_x=\begin{bmatrix}\left|\cos\left(\theta_{x1}\right)\right| & \left|\cos\left(\theta_{x2}\right)\right| & \cdots & \left|\cos\left(\theta_{xn}\right)\right|\\ \left|\sin\left(\theta_{x1}\right)\right| & \left|\sin\left(\theta_{x2}\right)\right| & \cdots & \left|\sin\left(\theta_{xn}\right)\right|\end{bmatrix}\quad(36)$$

$$\theta_{xy}=2\pi\times rand,x=1,2,\cdots,m;y=1,2,\cdots n\quad(37)$$

In equation: $P_x$ is the $x$ -th gene, and $\theta$ is the phase of the quantum bit; $m$ is the number of chromosomes; $n$ is the number of bits of the qubit, that is, the dimension of the solution space; $rand$ is a random number in the range $\left[0,1\right]$ .

(3) Quantum revolving gate

Quantum rotary gate is the key to complete the evolution of quantum genetic algorithm. The adjustment strategy of quantum rotary gate is adopted in this paper to compare the fitness $f\left(z\right)$ of the current individual with the fitness $f\left(best\right)$ of the optimal individual. If $f\left(z\right)<f\left(best\right)$ , the

probability amplitude $(\alpha, \beta)$ will change in the direction of $best$ ; if $f(z) > f(best)$ , the quantum bit at the corresponding position in $P_x$ will be adjusted accordingly, so that the probability amplitude $(\alpha, \beta)$ will change in the direction of $z$ . It should be noted here that the greater the difference between $f(z)$ and $f(best)$ , the greater the amplitude of the rotation angle of the quantum rotary gate to be changed; on the contrary, the smaller the amplitude of change.

Based on this theory, this paper adopts the adaptive rotation angle adjustment method of the quantum revolving door, as shown in (38):

$$\Delta\theta = \theta_{\min} + (\theta_{\max} - \theta_{\min}) \cdot \frac{\left| e^{f(best)} - e^{f(z)} \right|}{\left| e^{f(best)} \right|} \tag{38}$$

Where, $\theta_{\max}$ and $\theta_{\min}$ are the rotation angles of the maximum and minimum quantum rotary gates, respectively, and the rotation angle $\Delta\theta \in [0.001\pi, 0.05\pi]$ , so $\theta_{\min} = 0.001\pi, \theta_{\max} = 0.05\pi$ .

(4) Chromosomal variation

To avoid local optimum, this paper introduces the means of quantum mutation to operate chromosome mutation. The specific process can be divided into two steps: crossover and mutation:

Cross operation. Exchange the value of probability amplitude constant $(\alpha, \beta)$ to implement chromosome crossing. Because the number of gene exchanges between parent chromosomes required for single point crossing is large, which is easy to damage the current excellent population individuals, the method of double tangent point crossing is adopted here. This method has less gene exchanges for parent chromosomes involved in cross mutation, which can better retain the excellent population individuals.

Mutation operation. Generally, quantum bits always appear in pairs, so the probability amplitude constant $(\alpha, \beta)$ of each pair of quantum bits is taken as a whole, and part of the gene sequences in the current chromosome are changed randomly to achieve chromosome mutation.

The parameter settings of the quantum genetic algorithm are shown in Table I, the algorithm flow is illustrated in Fig.11.

TABLE I
ALGORITHM PARAMETER SETTINGS

| Parameter | MEANING | Value |
|---|---|---|
| $gen_{max}$ | Maximum population evolution algebra | 200 |
| $q_{popsize}$ | Quantum population number | 20 |
| $P_c$ | Crossover probability | 0.5 |
| $P_m$ | Mutation probability | 0.05 |
| $l_{chrom}$ | Chromosome length | 15 |

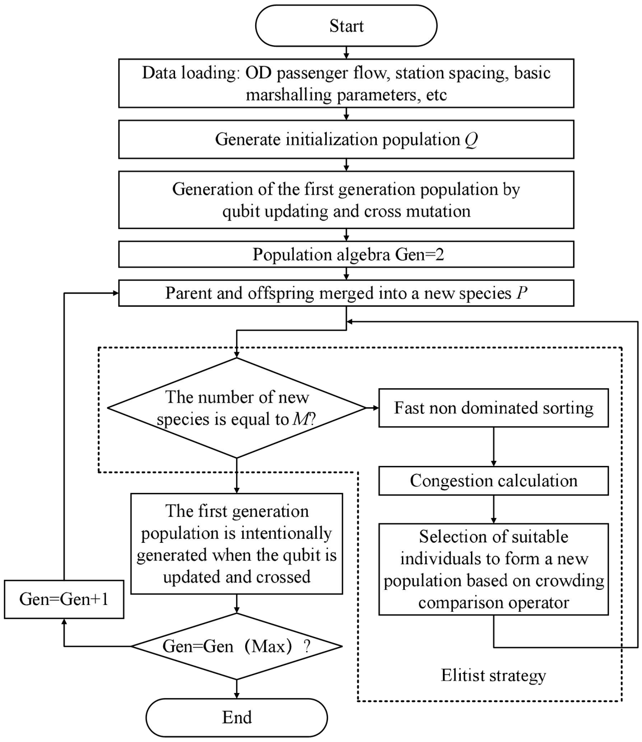


Fig.11. Algorithm Flow

## IV. CASE STUDY

### A. Case Background

To demonstrate the effectiveness of the model and algorithm, a real-world urban rail transit line is used as case study. There are 20 stations in the operation line, and the depot and the parking lot are connected to the starting and terminal stations. The starting and terminal stations and turn-back stations have the capability of reconnecting and unmarshalling. The parameter values are shown in Table II.

TABLE II
PARAMETER VALUES

| Symbol | Meaning | Value |
|---|---|---|
| $f_{\min}$ | Minimum departure frequency | 10 pairs/h |
| $f_{\max}$ | Maximum carrying capacity of the line | 30 pairs/h |
| $E$ | Vehicle capacity | 310 person |
| $N$ | Number of stations | 20 number |
| $V_d$ | Vehicle running speed (unified up and down) | 35 km/h |
| $T_z$ | Train turn back time | 110 s |
| $\lambda$ | Risk aversion coefficient | 2.25 |
| $g$ | Gravitational acceleration | 9.81 $m/s^2$ |
| $A$ | Empirical coefficient of basic resistance | 2.4 |
| $B$ | Empirical coefficient of basic resistance | 0.014 |
| $C$ | Empirical coefficient of basic resistance | 0.001293 |
| $\varpi_1$ | Train purchase cost | $3.9 \times 10^7$ yuan |
| $\varpi_2$ | Train operation cost | 8 yuan/km |
| $E_{k,e}$ | Average level of national power grid | 0.7 kg $CO_2e/kW \cdot h$ |

TABLE III

OPTIMAL OPERATION SCHEME

| Passenger flow section | Routing mode | Departure frequency (pairs/h) | | | | Passenger travel cost (yuan) | Enterprise operating cost (yuan) | Carbon emission (kg) | Turn back station position |
|---|---|---|---|---|---|---|---|---|---|
| | | Full-length routing | | Short-turn routing | | | | | |
| | | Large marshalling | Small marshalling | Large marshalling | Small marshalling | | | | |
| Morning peak | Single routing | 18 | 9 | 0 | 0 | 62540.84 | 30840.23 | 19762.85 | 9 — 16 |
| | full-length and short-turn routing | 16 | 6 | 8 | 6 | 74176.47 | 25766.46 | 17040.07 | |
| Flat peak | Single routing | 14 | 7 | 0 | 0 | 43932.46 | 17379.43 | 12425.40 | |
| | full-length and short-turn routing | 12 | 6 | 6 | 6 | 53942.45 | 14376.83 | 11425.44 | |
| Evening peak | Single routing | 16 | 8 | 0 | 0 | 67544.15 | 32541.23 | 20362.67 | |
| | full-length and short-turn routing | 14 | 7 | 7 | 6 | 76514.56 | 27586.46 | 18543.57 | |

Based on the multi-objective programming model constructed above, a quantum genetic algorithm is used to solve the problem on *Matlab*2021*a* , and relevant known parameters and classified passenger flows under different reconnection and unmarshalling schemes are substituted into the model for solution.

After that, the optimal matching departure frequency of large and small marshalling and full-length and short-turn routing, as well as the optimal values of each goal, are obtained. The iteration diagram of the quantum genetic algorithm is illustrated in Fig.12. The optimal results obtained are shown in Table III.

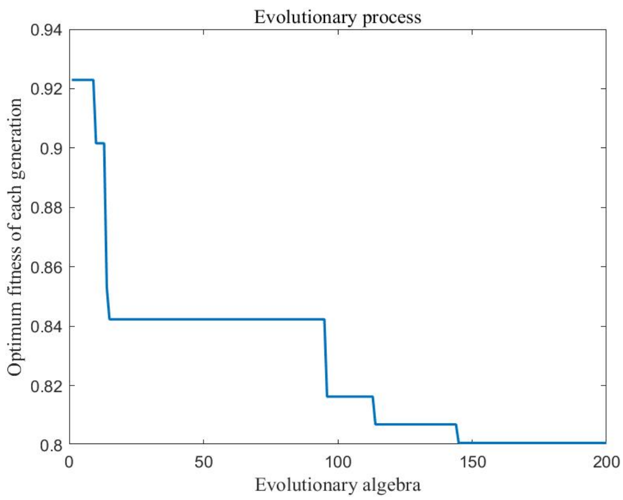


Fig.12. Iteration diagram of quantum genetic algorithm

*B. Discussion and analysis*

*B.1Comparison and analysis of full load ratio*

The balance of the full load ratio between large and small marshalling trains is one of the indicators reflecting the advantages and disadvantages of the train operation plan.

The quality of fixed marshalling plan and reconnection marshalling plan is compared and analyzed. The passenger flow demand and load factor of the section under the two marshalling plans are illustrated in Fig.13 and Fig.14.

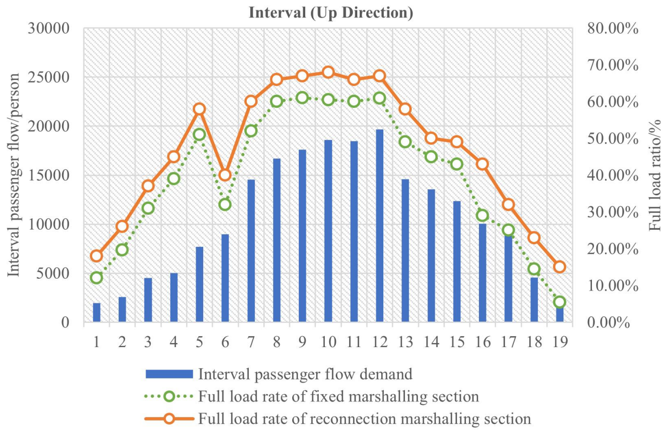


Fig.13. Comparison of full load rate between fixed marshalling and reconnection marshalling (Upward direction)

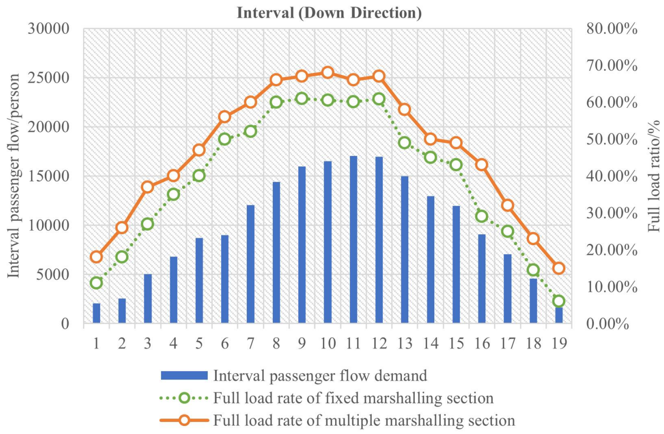


Fig.14. Comparison of full load rate between fixed marshalling and reconnection marshalling (Downward direction)

According to the analysis, the full load rate of the train reconnection marshalling plan in operation is 5%~10% higher than that of the fixed marshalling plan in operation. When designing the train marshalling plan for urban rail transit lines, the flexible organization form of the train marshalling plan in operation should be adopted as far as possible to improve the section full load rate, save the variable costs of enterprises, and then control the total cost of the entire urban rail transit system.

*B.2 Passenger flow transportation capacity of unit train set*

Compared with the fixed marshalling mode, the reconnection marshalling mode needs to consider the transportation capacity of the whole line section according to the number of unit trains. When the unit fleet reaches a specific number, the passenger flow transmission capacity of the section reaches its peak. The maximum transport capacity of passenger flow in each section varies with the number of units. The number of unit train sets can be determined according to the passenger flow in different sections. The matching relationship between the passenger flow transportation capacity and the number of unit vehicle groups is illustrated in Fig.15.

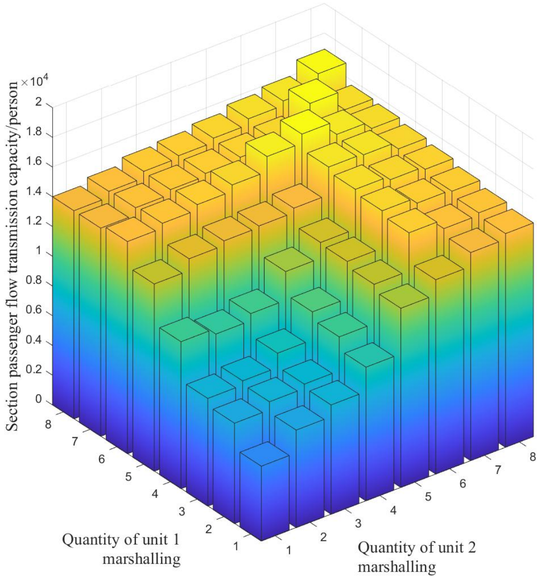


Fig.15. Matching relationship between inter district passenger flow transportation capacity and unit train set quantity

When the unit marshalling train reaches six car marshalling, the passenger flow transportation capacity in the section reaches the peak value and tends to be stable, and the transportation capacity remains unchanged even the number of marshalling vehicles increases.

*B.3 Analysis of travel time prospect value*

The impact on travel time of the change of income sensitivity coefficient $\sigma$ and loss sensitivity coefficient $\chi$.

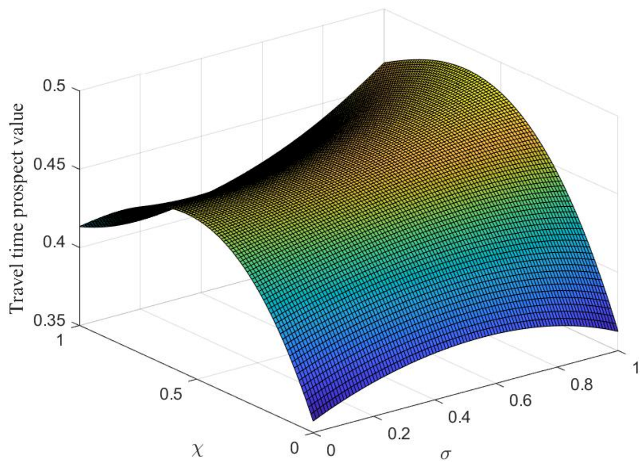


Fig.16. Prospect value of morning peak travel time

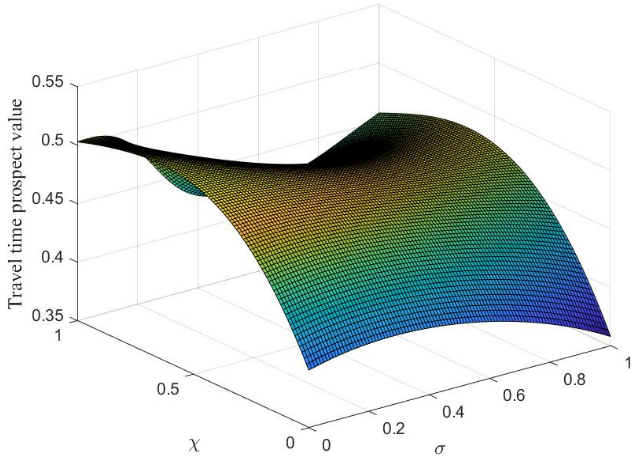


Fig.17. Prospect value of evening peak travel time

It can be seen from Fig.16 and Fig.17 that when $\sigma$ is constant, with the increase of $\chi$, the travel time prospect value first increases and then decreases. When $\chi$ is constant, the travel time prospect value increases with $\sigma$. In the early peak period, $\chi = 0.5$, the travel time prospect value reaches the peak. It shows that passengers are more sensitive to the loss of travel, which reflects the change of peak travel time in the morning and evening.

## V. CONCLUSION

Aiming at the optimization of train operation plans under the unbalanced spatiotemporal distribution of passenger flow in urban rail transit, a multi-objective optimization model for train operation plans under the reconnection train formation mode is constructed, and a quantum genetic algorithm solution model is designed to obtain the optimal solution set, and the ideal solution is selected as the optimal solution. The results show that:

First of all, the advantage of the train operation scheme with reconnection marshalling is that when the spatiotemporal imbalance of passenger flow is obvious, the passenger travel time cost can be reduced by adjusting the departure frequency and marshalling type, which can effectively reduce carbon emission and thereby achieve energy conservation and emission reduction.

Secondly, by comparing the comprehensive cost of reconnection marshalling and fixed marshalling schemes, it can be seen that when the time-space distribution of passenger flow demand in the line section is uneven, and the line is equipped with reconnection marshalling operation conditions, the full load rate of reconnection marshalling trains is higher than that of fixed marshalling trains, and the reconnection marshalling scheme is better. In the peak period, the train marshalling shall be mainly large marshalling, and the selection of train routing shall be appropriate to cover the section with high line load rate.

Finally, in order to reflect the characteristics of passenger travel, considering the limited rationality of passenger travel, the time prospect value is proposed to describe the relative travel time of passengers. It is reasonable and effective to introduce prospect theory to measure the travel time of passengers, so as to build an optimization model for the operation of reconnection marshalling.

In this paper, the train operation scheme of reconnection train formation is adopted, which effectively reduces carbon emissions, improves the sustainability of enterprise operation, attracts passengers to choose urban rail travel, and provides reference for the green and efficient train formation scheme of urban rail transit, which has guiding significance.

## REFERENCES


[1] Y.C. Tang, and B.R. Ma, “Research on flexible marshalling operation organization of urban rail transit,” *Journal of Railway Engineering Society*, vol. 31, no. 8, pp. 96-100, 2014.

[2] X.Y. Lei, G.F. Yang, C.Y. Yi, Q. Ma, and Y.J. Liu, “Discussion on the characteristics of flexible marshalling and combined transportation organization in rail transit,” *Railway Transport and Economy*, vol. 37, no. 9, pp. 64-69, 2015.

[3] D.D. Yu, B.M. Han, Q. Zhang, X.M. Yao, and F.L. Liu, “Optimization method of train operation scheme in rail transit based on flexible marshalling,” *Journal of Beijing Jiaotong University*, vol. 39, no. 6, pp. 21-31, 2015.

[4] G.Z. Bai, J. Guo, Y. Yang, and H.G. Shi, “Optimal Train Set Number Operation Scheme of Urban Rail Transit under Nesting Mode of Large and Small Routes,” *Research on Urban Rail Transit*, vol. 18, no. 3, pp. 45-50, 2015.

[5] H.M. Niu, X.S. Zhou, and R.H. Gao, “Train scheduling for minimizing passenger waiting time with time-dependent demand and skip-stop patterns: Nonlinear integer programming models with linear constraints,” *Transportation Research Part B*, vol. 76, pp. 117-135, 2015.

[6] Y.H. Wang, T. Tang, B. Ning, Ton J.J. van den Boom, and Bart De Schutter, “Passenger-demands-oriented train scheduling for an urban rail transit network,” *Transportation Research Part C*, vol. 60, pp. 1-23, 2015.

[7] P. Shang, R.M. Li, and L.Y. Yang, “Optimization of Urban Single-line Metro Timetable for Total Passenger Travel Time under Dynamic Passenger Demand,” *Procedia Engineering*, vol. 137, pp. 151-160, 2016.

[8] L.X. Yang, J.G. Qi, S.K. Li, and Y. Gao, “Collaborative optimization for train scheduling and train stop planning on high-speed railways,” *Omega*, vol. 64, pp. 57-76, 2016.

[9] J.Q. Liu, and N. Zhao, “Research on Energy-Saving Operation Strategy for Multiple Trains on the Urban Subway Line,” *Energies*, vol. 10, no. 12, pp. 2156, 2017.

[10] Y. Zhou, L.S. Zhou, Y. Wang, Z. Yang, and J.W. Wu, “Application of Multiple-Population Genetic Algorithm in Optimizing the Train-Set Circulation Plan Problem,” *Complexity*, vol. 2017, pp. 1-14, 2017.

[11] J.T. Yin, L.X. Yang, T. Tang, Z.Y. Gao, and B. Ran, “Dynamic passenger demand oriented metro train scheduling with energy-efficiency and waiting time minimization: Mixed-integer linear programming approaches,” *Transportation Research Part B*, vol. 97, pp. 182-213, 2017.

[12] Franca Rinaldi, and Romeo Rizzi, “Solving the train marshalling problem by inclusion–exclusion,” *Discrete Applied Mathematics*, vol. 217, pp. 685-690, 2017.

[13] J.L. He, R.Z. Zhang, X.J. Huang, and G.L. Xi, “Walking Access Distance of Metro Passengers and Relationship with Demographic Characteristics: A Case Study of Nanjing Metro,” *Chinese Geographical Science*, vol. 28, no. 4, pp. 612-623, 2018.

[14] C.J. Dai, Y.Z. Li, Z.S. Zhan, and H Chai, “Optimization of urban rail transit train operation plan considering dynamic passenger flow demand and large and small routing modes,” *China Railway Science*, vol. 39, no. 2, pp. 128-136, 2018.

[15] K.S. Fang, Q.Z. Dong, and H.X. Niu, “Study on the Optimization of Large and Small Routes of Urban Rail Transit under the Condition of Variable Marshalling,” *Railway Transport and Economy*, vol. 40, no. 5, pp. 94-99+110, 2018.

[16] D.H. Wang, and Q.G. Huang, “Application of Flexible Train Formation in Fully Automatic Operation Line of Urban Rail Transit,” *Research on Urban Rail Transit*, vol. 22, no. S2, pp. 102-105, 2019.

[17] J.P. Fang, Taku Fujiyama, and Howard Wong, “Modelling passenger distribution on metro platforms based on passengers’ choices for boarding cars,” *Transportation Planning and Technology*, vol. 42, no. 5, pp. 442-458, 2019.

[18] S.J. Li, R.H. Xu, and K. Han, “Demand-oriented train services optimization for a congested urban rail line: integrating short turning and heterogeneous headways,” *Transportmetrica A: Transport Science*, vol. 15, no. 2, pp. 1459-1486, 2019.

[19] W.Y. Chen, Y. Zhang, X. Chen, and J.Y. Wang, “Study on Cooperative Optimization of Operation Scheme of Large and Small Routes of Urban Rail Transit and Multi station Joint Current Limiting,” *Journal of Transportation System Engineering and Information Technology*, vol. 19, no. 5, pp. 177-184, 2019.

[20] Y.P. Rong, X.C. Zhang, Y. Bai, and D.J. Xu, “Study on Optimization of Operation Scheme of Multi marshalling Trains in Urban Rail Transit,” *Journal of Transportation System Engineering and Information Technology*, vol. 16, no. 5, pp. 117-122, 2016.

[21] Y.P. Rong, X.C. Qi, B. Li, and M. Liu, “Study on purchasing strategy of rail transit vehicles considering multi marshalling scheme,” *Journal of Transportation System Engineering and Information Technology*, vol. 17, no. 6, pp. 193-199+213, 2017.

[22] Y.P. Rong, “Research on the Method of Train Full Load Ratio Equalization Based on Multi marshalling,” *Journal of Transportation System Engineering and Information Technology*, vol. 19, no. 4, pp. 187-192+210, 2019.

[23] D.J. Xu, B.H. Mao, and L.G. Lei, “Study on Optimization of Train Operation Scheme for Large and Small Routes of Urban Rail Transit,” *Journal of Transportation System Engineering and Information Technology*, vol. 17, no. 1, pp. 120-126, 2017.

[24] D.J. Xu, J.W. Zeng, C.R. Ma, and S.K. Chen, “Study on Optimization of Train Operation Scheme for Large and Small Routes Considering Load Ratio Balance,” *Journal of Transportation System Engineering and Information Technology*, vol. 17, no. 6, pp. 185-192, 2017.

[25] D.J. Xu, B.H. Mao, S.K. Chen, L. Gong, and J.W. Zeng, “Optimization of Train Operation Scheme for Large and Small Routes Considering Running Proportion,” *Journal of Traffic and Transportation Engineering*, vol. 21, no. 2, pp. 173-186, 2021.

[26] Z.Y. Li, J. Zhao, and Q.Y. Peng, “Optimization of train routing plan for urban rail lines considering multi routing and multi formation,” *Journal of the China Railway Society*, vol. 42, no. 6, pp. 1-11, 2020.

[27] Q. Cheng, W. Deng, and Muhammad Ammar Raza, “Analysis of the departure time choices of metro passengers during peak hours,” *IET Intelligent Transport Systems*, vol. 14, no. 8, pp. 866-872, 2020.

[28] Y.L. Ye, J. Zhang, and Y.G. Wang, “Transfer Coordination-Based Train Organization for Small-Size Metro Networks,” *Arabian Journal for Science and Engineering*, vol. 45, no. 9, pp. 3599-3610, 2020.

[29] Y. Yan Tan, Z.B. Jiang, Y.X. Li, and R.X. Wang, “Integration of Train-Set Circulation and Adding Train Paths Problem Based on an Existing Cyclic Timetable,” *IEEE Access*, vol. 8, pp. 87142-87163, 2020.

[30] Z.C. Cao, Avishai (Avi) Ceder, D.W. Li, and S.L. Zhang, “Robust and optimized urban rail timetabling using a marshalling plan and skip-stop operation,” *Transportmetrica A: Transport Science*, vol. 16, no. 3, pp. 1217-1249, 2020.

[31] Hossein Falsafain, and Mohammad Tamannaei, “A Novel Dynamic Programming Approach to the Train Marshalling Problem,” *IEEE Transactions on Intelligent Transportation Systems*, vol. 21, no. 2, pp. 701-710, 2020.

[32] H.N. Fan, and Y.H. He, “Flexible train formation scheme and function realization of urban rail transit,” *Research on Urban Rail Transit*, vol. 24, no. 9, pp. 200-203, 2021.

[33] J.F. Yang, H. Wang, and J.G. Jin, “Optimization of Station-Skip in a Cyclic Express Subway Service,” *Networks and Spatial Economics*, vol. 24, no. 6, pp. 1-24, 2021.

[34] H.S. Zhou, J.G. Qi, L.X. Yang, J.G. Shi, and C.C. Gong, “Research on urban rail car bottom operation plan and robust passenger flow control strategy based on flexible marshalling,” *Control and Design*, 2022. DOI: https://doi.org/10.13195/j.kzyjc.2021.2054

[35] Q.W. Zeng, and Q.Y. Peng, “Study on the Cross line Operation Scheme of Urban Rail Trains Considering Multi marshalling,” *Journal of Railway Science and Engineering*, 2022. DOI: https://doi.org/10.19713/j.cnki.43-1423/u.T20220780

[36] J.G. Qi, H.S. Zhou, L.X. Yang, Y.R. Zhou, and C.T. Zhang, “Optimization of passenger and freight coordinated transportation scheme in rail transit under flexible marshalling,” *Journal of Transportation System Engineering and Information Technology*, vol. 22, no. 2, pp. 197-205, 2022.

[37] B. Jin, Y.X. Guo, Q.Y. Wang, P.F. Sun, and X.Y. Feng, “An Integrated Preparation Method of Timetable and Underbody Operation Plan Considering Large and Small Routes,” *China Railway Science*, vol. 43, no. 3, pp. 173-181, 2022.

[38] Y.Z. Dai, and S.G. Zhan, “Analysis of Large and Small Routing Schemes of Urban Rail Transit Considering Carbon Emission,” *Journal of Railway Science and Engineering*, vol. 19, no. 12, pp. 3546-3556, 2022.

[39] W.L. Zhou, Y. Huang, and L.B. Deng, “Urban rail timetable optimization considering operation energy saving and vehicle bottom

utilization," *Journal of Railway Science and Engineering*, 2022. DOI: https://doi.org/10.19713/j.cnki.43-1423/u.T20220474
[40] W.J. Sun, C.f. Zhu, and K.R. Liu, "Prospect Selection Decisions for Emergency Logistics Paths in Fuzzy Environments," *IAENG International Journal of Applied Mathematics*, vol. 53, no.1, pp. 183-193, 2023.
[41] K.Y. Chen, D. Zhou, Y.H. Su, H.B. Duan, and X.S. Chen, "Study on Carbon Emission Intensity and Potential of Urban Rail Transit in Life Cycle," *Railway Standard Design*, vol. 66, no. 5, pp. 1-7, 2022.
[42] Son Duy Dao, Kazem Abhary, and Romeo Marian, "Maximising Performance of Genetic Algorithm Solver in Matlab," *Engineering Letters*, vol. 24, no. 1, pp. 75-83, 2016.

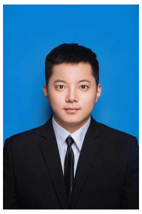

**Shixiang Wan** was born in Sichuan, China, in 1997. He obtained his Bachelor degree in Traffic and Transportation from Lanzhou Jiaotong University, Lanzhou, China, in the year 2021. He is currently pursuing his master degree in Traffic and Transportation (the Transportation Engineering) in Lanzhou Jiaotong University. His research interests include reconnection marshalling and the operation scheme.